

# Graphene oxide-COOH as a new saturable absorber for both Q-switching and mode-locking fiber lasers

Fengyan Zhao (赵凤艳)<sup>1,2</sup>, Yishan Wang (王屹山)<sup>1,\*</sup>, Yonggang Wang (王勇刚)<sup>3</sup>,  
Hushan Wang (王虎山)<sup>1,2</sup>, and Yajun Cai (蔡亚君)<sup>1,2</sup>

<sup>1</sup>State Key Laboratory of Transient Optics and Photonics, Xi'an Institute of Optics and Precision Mechanics,  
Chinese Academy of Sciences, Xi'an 710119, China

<sup>2</sup>University of Chinese Academy of Sciences, Beijing 100049, China

<sup>3</sup>School of Physics and Information Technology, Shaanxi Normal University, Xi'an 710119, China

\*Corresponding author: yshwang@opt.ac.cn

Received April 16, 2017; accepted June 6, 2017; posted online July 6, 2017

Graphene oxide carboxylic acid (COOH), a novel two-dimensional (2D) layered material with its unique optical and electronic properties, is discovered to exhibit the saturation of optical absorption under laser illumination. Applying the liquid-phase exfoliation method, we prepare graphene oxide-COOH dispersions with deionized water and fabricate graphene oxide-COOH polyvinyl alcohol polymer composite film. We further obtain stable Q-switching pulse and mode-locked laser operation with a 22.7 MHz repetition rate and a 1.5 ps pulse duration by incorporating the graphene oxide-COOH-based saturable absorbers into the all-fiber erbium-doped fiber laser cavity. The experimental results show that the proposed graphene oxide-COOH material can act as an effective absorber for pulsed fiber lasers, which demonstrate potential applications in the area of ultrafast optics.

OCIS codes: 140.4050, 140.3510, 140.3540, 160.4330.

doi: 10.3788/COL201715.101402.

Pulse laser sources have widespread applications, from basic research to telecommunications, material processing, sensing, medicine, frequency comb, and so on<sup>[1]</sup>. In order to achieve a pulse from picoseconds to femtosecond optical pulse, Q-switching and passively mode-locking based on saturable absorber (SA) are the widely used effective methods. As for the generation of the passively Q-switched and mode-locking pulses, it is very important to choose the SAs<sup>[2-5]</sup>. Therefore, ideal SAs with low saturation intensity, ultrafast recovery time, broadband operation bandwidth, and high damage threshold are the key topics in optics and photonics. Research on graphene opened up a door to two-dimensional (2D) nanomaterials, which possess a typical layered structure, where there exist a strong covalent bond in layers and a weak van der Waals interaction between layers<sup>[6]</sup>. Up to now, researchers have studied and developed graphene-like analogues of layered materials, such as carbon nanotubes (CNTs)<sup>[7]</sup>, topological isolators (TIs)<sup>[8]</sup>, molybdenum disulfide (MoS<sub>2</sub>)<sup>[9-13]</sup>, tungsten disulfide (WS<sub>2</sub>)<sup>[14,15]</sup>, and so on. Graphene and transition-metal dichalcogenides (TMDs) have been widely used as effective SAs in Q-switching, mode-locking fibers, and solid lasers due to inherent features of broad response and high flexibility. Unlike graphene 2D materials, layered semiconducting TMDs are direct band gap, which decreases with an increasing number of layers. Most recently, layered TMDs have been successfully synthesized and also been demonstrated for SAs. However, this kind of TMDs is limited, operating at the near-infrared (IR) and mid-IR range, due to their large bandgap near or in the visible region. Although introducing some suitable defects in the TMDs

could be applied as SAs in the IR and mid-IR region, the preparation process might become sophisticated. Graphene-based SAs have the advantages of ultrafast recovery time and broadband saturable sorption; however, the disadvantage of graphene is that it is insoluble in water. Though graphene is insoluble in water, it is also easily made into a graphene SA, realizing Q-switching and mode-locking pulse operation in all fiber lasers using this kind of SAs<sup>[16-20]</sup>. But, it is more complicated to fabricate graphene film than material, which has higher solubility in water. Therefore, deriving from the intensive research enthusiasm of graphene, there are a lot of derivatives of graphene, such as graphene oxide<sup>[21-25]</sup>, N-doped graphene, etc., which are applied to obtain Q-switching and mode-locking pulse in fiber and solid lasers due to it possessing of solubility<sup>[26]</sup>.

Currently, another rising 2D material, graphene oxide carboxylic acid (COOH), has attracted attention of researchers. Graphene oxide-COOH not only has the similar optical properties and structures of graphene and graphene oxide, but it also possesses its own new characteristics. Graphene oxide-COOH is a derivative of graphene, which is formed by graphene oxide breaking a covalent bond and adding a COOH group. Compared with graphene oxide, graphene oxide-COOH can be more easily dissolved in water due to its better hydrophilic nature. Such material has higher solubility than similar materials. Thus, it makes graphene oxide-COOH polyvinyl alcohol (PVA) film more convenient. Based on low saturation intensity and broadband SA, graphene oxide-COOH could also be used to obtain Q-switching or mode-locking operation in the IR and mid-IR region in fiber lasers.

Furthermore, the cost of this kind of SA is low, which makes it more attractive to researchers.

In this Letter, we demonstrate that Graphene oxide-COOH thin film has nonlinear SA property. We are able to obtain stable Q-switching and mode-locking operation by integrating this kind of thin film into an erbium-doped fiber (EDF) laser cavity. In the experiment, when the pump powers are varied from 25 to 40 mW, we realized a stable Q-switching operation state, and the repetition rate can be linearly changed in the range from 27.916 to 34.976 kHz, while the pulse width decreased from 12.292 to 5.536  $\mu$ s. When the pump power increased from 43 to 54.4 mW, a stable mode-locking state was also achieved. The repetition rate and the pulse duration were measured as 22.7 MHz and 1.5 ps, respectively. Our results suggest that graphene oxide-COOH material could be developed as an effective SA for ultrafast optics in practice.

The graphene oxide-COOH SA used in our experiment was exfoliated by the liquid-phase-exfoliation method, which has been used widely in the fabrication of 2D materials<sup>[27]</sup>. In our experiment, first, the solvent of graphene oxide-COOH flakes was dispersed in the deionized water. Then, the dispersion was sonicated for 180 min by 360 W ultrasonic cleaner to produce graphene oxide-COOH suspension. After sonication, the suspension was settled for several hours. In order to remove the residual graphene oxide-COOH flakes, the graphene oxide-COOH was centrifuged at 3000 rpm for 6 min. The upper supernatant with black color was harnessed in our experiment. The concentration of graphene oxide-COOH solution was 1 mg/mL. The inset of Fig. 1(a) shows the dispersion we obtain with black-purple color. The scanning electron microscopy (SEM) image in Fig. 1(a) illustrates the uniformity of graphene oxide-COOH SAs. We can see that this kind of 2D SA possesses irregular *f*.

After stabilizing for several days, we chose 5 wt% aqueous PVA solution and the graphene oxide-COOH solution for forming an SA film, which were mixed at the volume rate of 1:2. The mixture was stirred by a magnetic stirrer for 4 h and then dropped on a substrate. Lastly, a PVA-composite film was formed by evaporation under a certain temperature and pressure. A free standing SA film is then

fabricated with the easy method and can be adopted in the following experiments. We measured the Raman spectra of the graphene oxide-COOH nanosheets using an Ar laser at 532 nm. Figure 1(b) shows two main peaks of D and G located at 1330 and 1598  $\text{cm}^{-1}$ , respectively, on the Raman spectrum. The D peak came from a defect-induced breathing mode of  $\text{sp}^2$  rings. The G peak was caused by the double degenerate zone center  $E_{2g}$  mode<sup>[28]</sup>. The positions of two main Raman peaks are almost consistent with the previously reported results of graphene oxide. From the Raman spectra, we inferred that graphene oxide-COOH possesses better structure and symmetry compared to graphene oxide.

In order to investigate the characteristics of graphene oxide-COOH (SA), we measured the transmission using a homemade 1.5  $\mu\text{m}$  mode-locked fiber laser source. Figure 2(a) shows the picture in which graphene oxide-COOH-PVA is transferred to the end of the fiber connector. The nonlinear SA property is depicted in Fig. 2(b). The modulation depth and the saturable intensity inferred from the measured transmission curves are 3.5% and 1  $\text{MW}/\text{cm}^2$ , respectively.

Figure 3 shows the schematic diagram of an EDF laser, which is used to prove the SA property of the graphene oxide-COOH through the Q-switching and mode-locking operation state. The whole resonator consists of a 3.1 m EDF (LIEKKI Er 80- 8/125) with an absorption coefficient of 4.5 dB/m at 980 nm, a wavelength-division multiplexer (WDM), a polarization controller (PC), a polarization-independent isolator, and an optical coupler with an output ratio of 10%. A 980 nm laser diode source is coupled into the ring cavity through a 980/1550 nm wavelength-division multiplexer. The polarization-independent isolator is utilized to realize unidirectional operation of the laser cavity. An optical coupler with an output ratio of 10% is utilized to extract output power from the laser ring cavity. The total length of the ring resonator is 9.1 m. The dispersion parameters  $D$  at 1.55  $\mu\text{m}$  for the EDF and single mode fiber (SMF) are  $-16$  and  $17$   $\text{ps}/(\text{nm} \cdot \text{km})$ , respectively. Therefore, the net dispersion of our fiber cavity is calculated to be  $-0.0671$   $\text{ps}^2$ . Our oscillation cavity in this case tends to be a shaped soliton-like

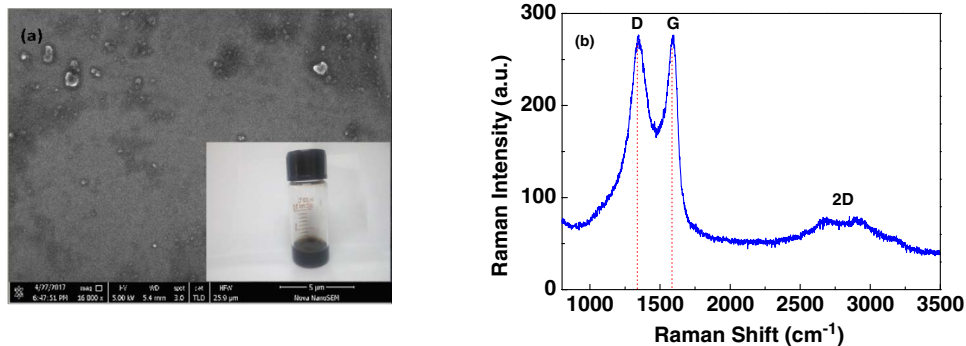


Fig. 1. Characterization of graphene oxide-COOH nanosheets. (a) SEM image, the inset shows graphene oxide-COOH solution; (b) Raman spectra.

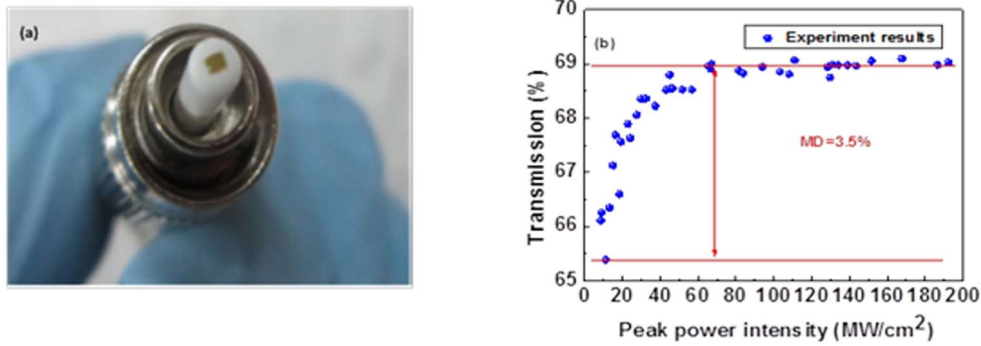


Fig. 2. (a) Graphene oxide-COOH-PVA film attached on the end of fiber connector; (b) nonlinear transmission curve of graphene oxide-COOH-PVA film.

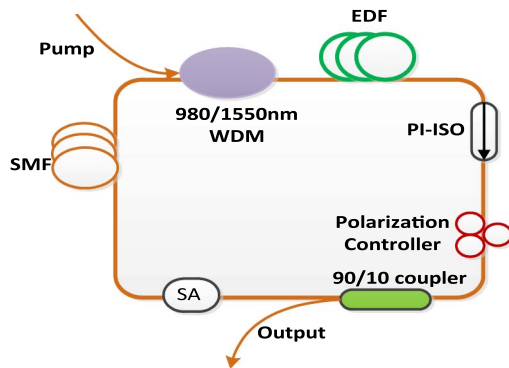


Fig. 3. Experimental setup of the fiber laser with graphene oxide-COOH as a mode locker.

pulse, which originates from the interaction between self-phase modulation and the anomalous group velocity dispersion.

In the experiment, the graphene oxide-COOH-PVA film with a concentration of 1 mg/mL was placed on the facet of the fiber connector in the ring EDF cavity mentioned above. Continuous wave (CW) emission was achieved by increasing the incident pump power up to 10 mW. A self-started Q-switching state was obtained when the incident power changed from 10 to 20 mW. A stable Q-switching state could be maintained when the pump power increased from 20 to 40 mW. The threshold is lower than those previously reported results based on the graphene oxide<sup>[28]</sup>. Moreover, our experimental results showed that Q-switching pulse operation is not affected by the tuning position of the PC. We use a fast photo-detector with a working wavelength range of 1.1–1.7  $\mu\text{m}$  to record the Q-switching pulse train, and the corresponding results were displayed in a digital oscilloscope with a bandwidth of 1 GHz (Tektronix TDS3024C). Figure 4 summarizes the Q-switching laser performance. Figure 4(a) shows the pulse trains, which indicate that the output repetition rate and pulse duration are 34.976 kHz and 5.536  $\mu\text{s}$ , respectively. There is no peak intensity modulation observed demonstrating the high stability of the Q-switching state. The output repetition

rate and pulse duration are dependent on pump power, as depicted in Fig. 4(b). In this case, as expected, when the pump power is boosted, the repetition rate increases and the pulse duration decreases. When we further boost the pump power, the repetition rate increases almost linearly from 27.916 to 34.976 kHz, while the pulse duration varies from 12.292 to 5.536  $\mu\text{s}$ . Meanwhile, the output power and pulse energy are measured in our cavity, and the results are displayed in Fig. 4(c). As shown in the figure, the output power and pulse energy increase with the increase of the incident power. Furthermore, the average output power rises linearly with the pump power. When the pump power reaches 40 mW, we obtain the maximum output power of 760  $\mu\text{W}$  from our laser cavity, corresponding to an output pulse energy of 23.7 nJ. Noting that the output performance of the results in our experiment is comparable to those achieved in EDF lasers with other kinds of absorber materials (e.g., CNTs, black phosphorus, and graphene)<sup>[29,30]</sup>. The measured optical spectrum is shown in Fig. 4(d). The center wavelength locates at 1559.7 nm and the 3 dB spectral bandwidth of the Q-switching strains is 1 nm.

When the pump power exceeds 40 mW, the Q-switched pulse train becomes unstable. However, when the pump power further reaches 43 mW, the mode-locking state suddenly appears. Moreover, the output power is around 1 mW for the pump power of 54.4 mW. Compared with the typical performance of mode-locked EDF lasers using a graphene oxide SA, the threshold is lower, and the efficiency is higher. Thus, we could consider that graphene oxide-COOH contributes to the higher efficiency of our laser resonator. We found that the mode-locking was virtually independent of the tuned position of the PC. Figure 5 summarizes the performance of the mode-locking operation for a pump power of 54.4 mW in the fiber laser cavity. As shown in Fig. 5(a), in typical Kelly spectral sidebands, the center wavelength locates at 1559.6 nm with a 3 dB spectral bandwidth of 1.85 nm. Although we obtained the mode-locking operation state, the asymmetry profile and the unsmooth spectrum indicate that some CW noises exist in the ring oscillator along with the intracavity soliton.

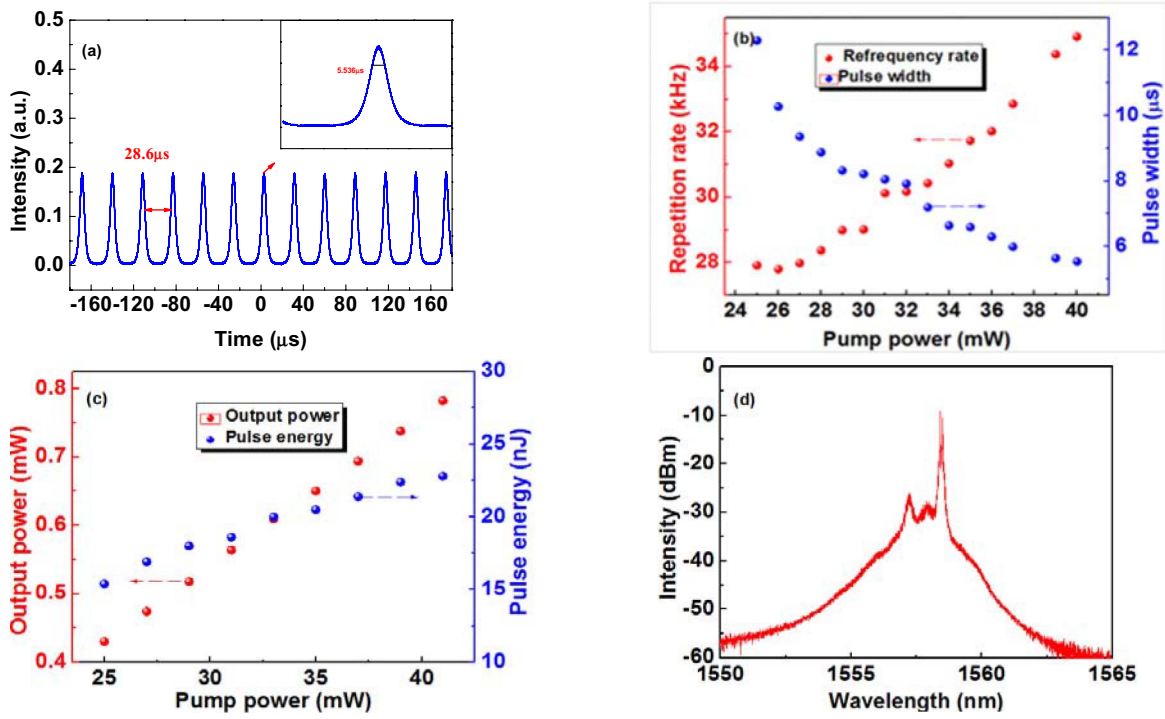


Fig. 4. (Color online) (a) Pulse trains at the pump power of 40 mW; inset, single pulse profile of the Q-switching laser; (b) the evolution of pulse repetition rate and duration as pump power increases; (c) the evolution of output power and pulse energy with the pump power; (d) the output spectrum of Q-switching.

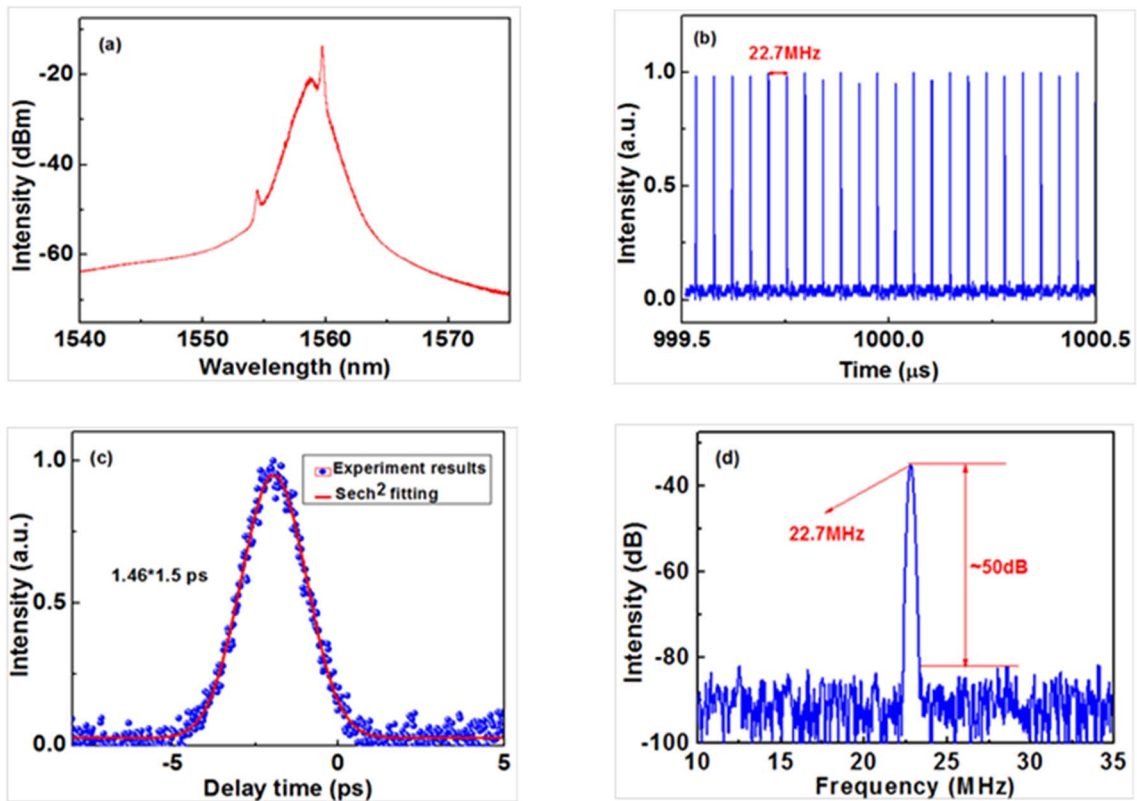


Fig. 5. (a) Output spectrum of mode-locking pulse; (b) output pulse train; (c) output autocorrelation trace with a pulse duration of 1.5 ps; (d) radio-frequency spectrum.



Figure 5(b) exhibits the output pulse train of the mode-locked laser. The period is 44.1 ns, corresponding to a repetition rate of 22.7 MHz, which matches well with the total fiber cavity length of 9.1 m. Figure 5(c) shows the measured autocorrelation trace that can be well fitted by a  $\text{sech}^2$  profile. The output pulse duration is about 1.5 ps, corresponding to a time-bandwidth product that is 0.34, which is close to the value of 0.315 in a transform-limited case. In order to investigate the stability of the mode-locking state, we also record the radio frequency spectrum at the fundamental repetition rate of 22.7 MHz, as shown in Fig. 5(d). The signal-to-noise ratio (SNR) is smaller than 50 dB. We notice that, actually, the SNR for a mode-locking EDF laser can reach as high as 80 dB if semiconductor SA mirror (SESAM) is utilized<sup>[31]</sup>. Therefore, we infer that a lower SNR could be because, as an absorber, the quality of graphene oxide-COOH is still not perfect. During the fabrication of graphene oxide-COOH SAs, the shorter the sonication time is, the lower the solubility is, so a proper sonication time would improve the solubility of this kind of SAs, which will increase the SNR. We also consider that a CW also exists and circulates in our cavity, which also results in the decrease of the SNR.

In order to verify whether the Q-switching or mode-locking operation is caused by the effect of graphene oxide-COOH-PVA film applied in our cavity, the fiber laser is operated in the same laser cavity without the incorporation of a graphene oxide-COOH SA. No matter how the pump power and the cavity polarization state are adjusted, no Q-switching or mode-locking pulse forms in our cavity. Therefore, we conclude that the mode-locking operation is caused by the graphene oxide-COOH.

In conclusion, we verify that graphene oxide-COOH can be formed as an effective SA for the mode-locking operation. The measured transmission curve clearly shows that graphene oxide-COOH possesses an obvious SA property. In our experiment, we successfully demonstrate that the Q-switching or mode-locking operation can be achieved by using the graphene oxide-COOH SA in the ring EDF laser. We obtain stable Q-switched laser operations with the shortest pulse duration of 5.536  $\mu\text{s}$ , corresponding to pulse repetition rate of 34.9 kHz. Furthermore, a stable mode-locking pulse is achieved with a pulse width of 1.5 ps by increasing the pump power in the fiber laser. To the best of our knowledge, it is the first time realizing a Q-switched and mode-locked pulse in the fiber laser with graphene oxide-COOH-PVA film. Our experimental results show that graphene oxide-COOH could be a new 2D material and adopted as a mode locker. The results indicate that graphene oxide-COOH has potential applications in the mid-IR wave range.

This work was supported by the National Natural Science Foundation of China (No. 61690222) and the CAS/SAFEA international Partnership Program for creative Research Teams.

## References

1. M. E. Ferman, A. Galvanauskas, and G. Sucha, *Ultrafast Lasers Technology and Applications* (Marcel Dekker, 2003).
2. A. Martinez and Z. Sun, *Nat. Photon.* **7**, 842 (2013).
3. Z. Luo, M. Zhou, J. Weng, G. Huang, H. Xu, and C. Zhao, *Opt. Lett.* **35**, 3709 (2010).
4. Z. P. Sun, T. Hasan, F. Torrisi, D. Popa, G. Provotera, and F. Q. Wang, *ACS Nano* **4**, 803 (2010).
5. K. F. Mak, M. Y. Sfeir, Y. Wu, C. H. Lui, J. A. Misewich, and T. F. Heinz, *Phys. Rev. Lett.* **101**, 196405 (2008).
6. H. Zhang, Q. Bao, D. Tang, L. Zhao, and K. Loh, *Appl. Phys. Lett.* **95**, 141103 (2009).
7. J. W. Nicholson, R. S. Windeler, and D. J. DiGiovanni, *Opt. Express* **15**, 9176 (2007).
8. M. Liu, N. Zhao, H. Liu, and X. W. Zheng, *IEEE Photon. Technol. Lett.* **26**, 983 (2014).
9. H. Zhang, S. B. Lu, J. Du, S. C. Wen, D. Y. Tang, and K. P. Loh, *Opt. Express* **22**, 7249 (2014).
10. R. I. Woodward, R. C. T. Howe, T. H. Runcorn, G. Hu, F. Torrisi, E. J. R. Kelleher, and T. Hasan, *Opt. Express* **23**, 20051 (2015).
11. H. D. Xia, H. P. Li, C. Y. Lan, C. Li, X. X. Zhang, S. J. Zhang, and Y. Liu, *Opt. Express* **22**, 17341 (2014).
12. R. Khazaiezhad, S. H. Kassani, H. Jeong, D.-I. Yeom, and K. Oh, *Opt. Express* **22**, 23732 (2014).
13. X. Zou, Y. Leng, Y. Li, Y. Feng, P. Zhang, Y. Hang, and J. Wang, *Chin. Opt. Lett.* **13**, 081405 (2015).
14. D. Mao, Y. Wang, C. Ma, L. Han, B. Jiang, X. Gan, S. Hua, W. Zhang, T. Mei, and J. Zhao, *Sci. Rep.* **5**, 7965 (2015).
15. W. Liu, L. Pang, H. Han, Z. Shen, M. Lei, H. Teng, and Z. Wei, *Photon. Res.* **4**, 111 (2016).
16. S. Xu, J. Zhan, B. Man, S. Jiang, W. Yue, S. Gao, C. Gou, H. Liu, Z. Li, J. Wang, and Y. Zhou, *Nat. Commun.* **8**, 14902 (2017).
17. S. C. Xu, B. Y. Man, S. Z. Jiang, C. S. Chen, C. Yang, M. Liu, Q. J. Huang, C. Zhang, D. Bi, X. Meng, and F. Y. Liu, *Opt. Laser Technol.* **56**, 393 (2014).
18. X.-L. Li, J.-L. Xu, Y.-Z. Wu, J.-L. He, and X.-P. Hao, *Opt. Express* **19**, 9950 (2011).
19. S. C. Xu, B. Y. Man, S. Z. Jiang, D. J. Feng, S. B. Gao, C. S. Chen, M. Liu, C. Yang, D. Bi, F. Y. Liu, and X. Meng, *Opt. Lett.* **39**, 2707 (2014).
20. S. C. Xu, B. Y. Man, S. Z. Jiang, C. S. Chen, C. Yang, M. Liu, X. G. Gao, Z. C. Sun, and C. Zhang, *Appl. Phys. Lett.* **102**, 151902 (2013).
21. S. Huang, Y. Wang, P. Yan, J. Zhao, H. Li, and R. Lin, *Opt. Express* **22**, 11417 (2014).
22. J. Liu, Y. G. Wang, Z. S. Qu, L. H. Zheng, L. B. Su, and J. Xu, *Laser Phys. Lett.* **9**, 15 (2012).
23. Y. Wang, Z. Qu, J. Liu, and Y. H. Tsang, *IEEE J. Lightwave Technol.* **30**, 3259 (2012).
24. C. Zuo, J. Hou, B. Zhang, and J. He, *Chin. Opt. Lett.* **13**, 021401 (2015).
25. Y. G. Wang, H. R. Chen, X. M. Wen, W. F. Hsieh, and J. Tang, *Nanotechnology* **22**, 455203 (2011).
26. Y. W. Song, S. Y. Jang, W. S. Han, and M. K. Bae, *Appl. Phys. Lett.* **96**, 051122 (2010).
27. Y. Hernandez, V. Nicolosi, F. M. Blighe, J. Hutchison, V. Scardaci, A. C. Ferrari, and J. N. Coleman, *Nat. Nanotechnol.* **3**, 563 (2008).
28. J. Zhao, Y. Wang, S. Ruan, P. Yan, H. Zhang, Y. H. Tsang, J. Yang, and G. Huang, *J. Opt. Soc. Am. B.* **31**, 716 (2014).
29. S. Y. Choi, H. Jeong, B. H. Hong, F. Rotermund, and D.I. Yeom, *Laser Phys. Lett.* **11**, 015101 (2014).
30. D. Li, H. Jussila, L. Karvonen, J. Lipsanen, X. Chen, and Z. Sun, *Physics* **5**, 15899 (2015).
31. Q. Wang, T. Chen, B. Zhang, M. Li, and Y. Lu, *Appl. Phys. Lett.* **102**, 13117 (2013).